Food Hydrocolloids 101 (2020) 105536

Contents lists available at ScienceDirect

Food Hydrocolloids

journal homepage: http://www.elsevier.com/locate/foodhyd

Gelling mechanism of RG-I enriched citrus pectin: Role of arabinose side-chains in cation- and acid-induced gelation

Jiaqi Zheng [a], Jianle Chen [a], Hua Zhang [a], Dongmei Wu [a], Xingqian Ye [a], Robert J. Linardt [b], Shiguo Chen [a,*]

[a] College of Biosystems Engineering and Food Science, Zhejiang Key Laboratory for Agro-Food Processing, Department of Food Science and Nutrition, Zhejiang University, Hangzhou, 310058, China

[b] Center for Biotechnology & Interdisciplinary Studies, Department of Chemistry & Chemical Biology, Rensselaer Polytechnic Institute, Biotechnology Center 4005, Troy, NY, 12180, USA

ARTICLE INFO

Keywords:
Pectin
Rhamnogalacturonan-I
Side-chains
Gelling

ABSTRACT

RG-I enriched pectin is present in fruit and vegetable containing products. However, it is removed by the hot acid treatment during commercial pectin production to improve gelling properties and to afford a more uniform pectin quality. Recently, an awareness of the health benefits of RG-I enriched pectin has caused technologists to rethink its utilization by the food industry, especially as a novel healthy gelling agent. Unique RG-I enriched pectin with abundant arabinan side-chains was extracted from citrus membrane by sequential mild acidic and alkaline treatment. Arabinose was then removed by enzymatic treatment to investigate the impact of arabinose side-chains on gelation. The properties of RG-I enriched pectin gels, prepared using cations or acid, showed it could form gels under conditions required for both low and high methoxyl pectin as a result of its highly branched structure. In cation-induced gelation, the HG region forms egg-box junction zones with divalent cations and the side-chains of the RG-I region stabilizes the network structure through entanglements. In acid-induced gelation, low pH promotes formation of hydrogen bonding and hydrophobic interactions within the HG region and the side-chains create a tighter conformation, eventually allowing for stronger interactions between the pectin chains.

1. Introduction

Pectin, the most complex and widely distributed polysaccharide from plant cell walls, is composed of linear homogalacturonan (HG), rhamnogalacturonan-I (RG-I), rhamnogalacturonan-II (RG-II) and other substituted galacturonans including XGA. HG is a linear chain of galacturonic acid residues and called "smooth region". RG-I is called "hairy region" with a backbone consisting of the repeating alternative rhamnose and galacturonic acid residues, branched with diverse types of neutral side-chains (Yapo, 2011). It is widely used as a thickener and gelling agent in the food, pharmaceutical and cosmetics industry. Commercial pectins are mainly produced from citrus peel and apple pomace, and are HG-dominated, the result of removing the RG-I region under harsh hot acid conditions to achieve better gelling properties and quality control (Sandarani, 2017). Based on the degree of methoxylation (DM), commercial pectins are classified as high-methoxylated pectin (HMP) (DM $>$ 50%) or low-methoxylated pectin (LMP) (DM $<$ 50%). HMP forms gels at low pH with high sucrose concentrations and LMP forms gels in presence of cations and these properties are important for producing diverse gelling food such as jams, jellies (HMP gels) and low-calorie jellies (LMP gels). Recently, scientists have realized that the neutral sugar side-chains, removed in pectin production, have a variety of important bioactivities, including inhibition of cell migration, immunological activities and prebiotic activities (Babbar, Dejonghe, Gatti, Sforza, & Elst, 2016; Wu et al., 2019). In particular, the side-chains of the RG-I region can bind to the carbohydrate recognition domain (CRD) on the pro-metastatic protein galectin-3 (Gal 3) (Gunning, & Bongaerts, and Morris, 2009; Zhao et al., 2017). Such binding inhibits its ability to promote cell adhesion and migration, thus, reducing the risks of the onset of cancer (Kapoor & Dharmesh, 2017; Li, & Yang, & Li, and Feng, 2018; Maxwell, & Belshaw, & Waldron, and Morris, 2012). The awareness of the functionality of these neutral sugar side-chains has led us to reconsider widely used methods for the pectin extraction.

* Corresponding author.
E-mail address: chenshiguo210@163.com (S. Chen).

https://doi.org/10.1016/j.foodhyd.2019.105536
Received 7 August 2019; Received in revised form 31 October 2019; Accepted 21 November 2019
Available online 22 November 2019

A number of mild extraction methods using acid and alkaline have been reported to retain the RG-I region, although the different condition resulted in total different structure. RG-I content of sugar beet pectin extracted at pH 2 and 80 °C was 34% while it was only 7% at pH 1.5 and 90 °C, therefore pH and temperature were the main parameters influencing the ratio of RG-I and HG (Yapo, & Robert, & Etienne, & Wathelet, and Paquot, 2007). To avoid the hydrolysis of the neutral sugar side chains and the acid-labile linkages between the GalA and Rha residues in the RG-I region, alkali methods are usually used for RG-I enriched pectin extraction. A low-temperature alkali treatment in 1 M NaOH solution has been used to extract a pectic polysaccharide containing 72% RG-I from pumpkin (Zhao et al., 2017). Alkaline and enzyme-assisted alkaline extraction methods in 1.5 M KOH solution were compared and the pectin obtained using combined alkali-enzymatic method contained more RG-I (85%) than alkali extracted pectin (80%). However, most of these methods are in laboratory stage and difficult to implement at large scale (Khodaei and Karboune, 2013, 2014). In our previous research, a novel low methoxyl RG-I enriched pectin was extracted from citrus canning processing water by sequential acid and alkaline treatment of the segment membrane. This pectin maintained its capability of gelling in the presence of Ca^{2+} without the addition of sucrose while containing relatively low GalA content (Chen et al., 2017; Zhang et al., 2017). However, the mechanism of gelation of this RG-I enriched pectin is still unclear.

Past research has mainly focused on the influence of HG structural features on the rheological characteristics of pectin gels (Fraeye, & Duvetter, & Doungla, & Van Loey, and Hendrickx, 2010; Willats, & Knox, and Mikkelsen, 2006) but rarely on the impact of the highly branched RG-I regions. Recently, the gelation properties of RG-I enriched pectins extracted from various sources have been reported providing a new perspective for the development of functional food hydrocolloids. RG-I backbone is not compatible with the gel formation because the rhamnose inserts on the homogalacturonan chain produce “kinks” in the backbone, thereby, limiting cross-linking. However, the neutral sugar side-chains of the RG-I region reportedly possess strong water-binding capacities and stabilize the network structures in both cation- and acid-induced gels (Makshakova, & Faizullin, & Mikshina, & Gorshkova, and Zuev, 2018; Mikshina et al., 2017; Ngouémazong et al., 2012; Schmelter, & Wientjes, & Vreeker, and Klaffke, 2002; Sousa, & Nielsen, & Armagan, & Larsen, and Sørensen, 2015). The novel highly branched structure of RG-I enriched pectin shows potential for gelation applications. RG-I enriched pectin has a synergistic effect on the gelation of traditional commercial pectins and other polysaccharides. RG-I pectin, with long galactan side branches extracted from okra, reduced the sucrose content required for gelation and acted as a synergistic gel for high-methoxyl pectin. Side-chain entanglements create a pliable and continuous network, thus, these blended gels show excellent toughness and high fracture strain (Chen et al., 2019; Li et al., 2019). RG-I enriched pectin has also been used for drug delivery and the high RG-I branching structure causes enhanced gastric and small intestinal resistance of Ca^{2+}-pectin beads and can be applied as the carriers for the colon delivery of drugs (Günter, & Popeyko, and Istomina, 2019). All of this research suggests RG-I has unique gelation properties and potential applications in functional food hydrocolloids, but fails to explain the mechanism of gelation and the structure-function relations of RG-I enriched pectin gels.

Thus, the aim of this research is to describe the effects of neutral sugar side-chains on the rheological properties of RG-I enriched pectin gels in both cation- and acid-induced gelation. The RG-I enriched citrus pectin (CP) and enzymatically de-branched citrus pectins (DCP) were prepared and their gelling properties were compared to establish a comprehensive structure-function relationship for these pectins.

2. Materials and methods

2.1. Materials

Citrus pectin (CP) sample was recovered from basic water discharged from citrus canning factories during the segment membrane removal process, including two-step filtration, concentration and ethanol precipitation. The basic water underwent pH-adjustment to neutral and precipitation with 95% ethanol in the volume ratio of 1:1. After precipitation, precipitates were washed with 95% ethanol 3 times to remove salt and oven-dried at 55 °C for 24 h. An endo-α-1,5-arabinanase [EC 3.2.1.99], originating from *Aspergillus niger*, was purchased from Megazyme (UK). Monosaccharide standards, 1- phenyl-3-methyl-5-pyrazolone (PMP) and D_2O were all purchased from Sigma-Aldrich (Shanghai, China). All other chemicals used were of analytical grade.

2.2. Pectin de-branching

Controlled enzymatic de-branching of pectin was performed by incubation with endo-α-1,5-arabinanase (Ngouémazong et al., 2012; Sousa, Nielsen, Armagan, Larsen, & Sørensen, 2015). Pectin to be treated was solubilized in 0.1 M sodium acetate pH 4.0 to a final concentration of 0.2% (w/v). For 100 mL of pectin solution either no enzyme (control) or 15 U of enzyme was added. The solutions were incubated for 48 h at 40 °C with continuous agitation. After incubation, the solutions were maintained at 85 °C for 4 min to inactivate the enzyme and then rapidly cooled in an ice bath. The solution was adjusted to pH 7.0 and dialyzed (MWCO 10 kDa) against de-mineralized water for 48 h to remove sodium salts and oligosaccharides from the partially de-branched pectin samples. Na^+ content may be slightly different between CP and DCP after dialysis due to different structure, but the difference has little effect on viscosity and viscoelastic properties of pectin solutions (Barbieri et al., 2019). Dialyzed samples were then lyophilized and stored.

2.3. Determination of chemical composition

Monosaccharide composition was analyzed by a modified 1-phenyl-3-methyl-5-pyrazolone (PMP)-high performance liquid chromatography (HPLC) method (Strydom, 1994). First, pectic polysaccharides samples (typically 2–3 mg) were hydrolyzed with 2 M trifluoroacetic acid at 110 °C for 8 h in an ampoule. Then, the samples were dried using a stream of nitrogen and neutralized with 0.1 M sodium hydroxide. The hydrolyzates dissolved in 450 mL of 0.3 M sodium hydroxide were derivatized with 450 mL PMP solution (0.5 M, in methanol) at 70 °C for 30 min. Finally, the reaction was stopped by neutralization with 0.3 M hydrochloric acid, and excess reagent was extracted using 3 × 1 mL of chloroform. The upper (aqueous) phase was filtered through a 0.22 mm membrane and 1 mL of the resulting solution was injected for analysis. Waters e2695 (Waters, US) with a Zorbax Eclipse XDB-C18 column (250 mm 4.6 mm, 5 mm, Agilent, USA) was used to perform HPLC analysis at 25 °C. The mobile phases were: solvent A, 15% acetonitrile with potassium phosphate buffer (0.05 M, pH 6.9), solvent B, 40% acetonitrile with the same buffer. The flow rate was 1 mL/min, relying on a gradient of B from 0% to 15% in the initial 10 min, then from 15% to 25% in the next 20 min. Detection was with a 2489 UV/Vis Detector (Waters, US) at 250 nm.

The degree of methylation (DM) was analyzed by the m-phenylphenol method calculated from methanol and acetic acid content with the GalA%. Pectins after saponification were used to determine methanol and acetic acid content by HPLC (Waters 1525, US) with a C18 column (SinoChrom ODS-BP 250 mm × 4.6 mm, 5 mm, Elite, China) with refractive index (RI) detection (Waters 2414, US) using isopropanol as internal standard and the mobile phase was 4 mM sulfuric acid (Levigne, & Thomas, & Ralet, & Quemener, and Thibault, 2002).

Table 1
Chemical composition and molecular weight of pectin.

	Monosaccharides (mol%)								Rha/GalA	RG-I%[a]	(Ara + Gal)/Rha[b]	DM%[c]	DAc %[d]	Mw[e] (kDa)	Rz[f] (mm)
	Man	Rha	GalA	Glc	Gal	Xyl	Ara	Fuc							
CP	3.20 ± 0.11[a]	4.19 ± 0.09[a]	23.47 ± 0.20[a]	0.35 ± 0.01[a]	11.05 ± 0.04[a]	12.82 ± 0.11[b]	43.27 ± 0.26[b]	1.28 ± 0.27[a]	0.18 ± 0.00[a]	62.70 ± 0.04[b]	12.96 ± 0.33[b]	15.06 ± 0.16[b]	0.83 ± 0.09[a]	282.7 (±2.5%)[b]	36.6 (±6.7%)[a]
DCP	4.67 ± 0.29[b]	6.85 ± 0.12[b]	42.42 ± 0.40[b]	0.94 ± 0.50[a]	17.03 ± 0.67[b]	6.43 ± 0.77[a]	20.52 ± 0.34[a]	1.15 ± 0.73[a]	0.16 ± 0.00[a]	51.25 ± 0.77[a]	5.48 ± 0.24[a]	13.09 ± 0.35[a]	0.40 ± 0.07[a]	175.2 (±1.3%)[a]	36.2 (±3.3%)[a]

[a] RG-I% = 2Rha% + Ara% + Gal%.
[b] (Ara + Gal)/Rha: average length of RG-I side chains.
[c] DM: degree of methylation.
[d] DAc: degree of acetylation.
[e] Mw: weight-average of molar mass.
[f] Rz: z-average of root mean square radius of gyration.

2.4. Nuclear magnetic resonance (NMR) analysis

Pectin samples (5 mg) for NMR analysis were replaced exchangeable protons by lyophilization twice from deuterium oxide and then dispersed in 0.5 mL of D_2O (99.96%). The NMR spectra were recorded on Agilent DD2-600 MHz spectrometer (Agilent Technologies, Santa Clara, CA, USA) at 25 °C.

2.5. SEC-MALLS analysis

Size exclusion columns including a OHpak SB-G guard column, SB-806 HQ and SB-804 HQ column (Shodex, Japan), equipped with a multi-angle laser light scattering detector (DAWN HELEOS II, Wyatt Technology, USA), a viscometer (ViscoStarTM III, Wyatt Technology, USA) and refractive index detector (SEC-MALLS-VISC-RI) were applied to provide molecular weight information on the pectins. The molar mass was calculated using specific refractive index increment at 0.0880 mL/g for pectins (Chen et al., 2017) and result of dn/dc value measurement was shown in supplementary data. Pectins were dissolved in H_2O (3 mg/mL) and filtered through 0.22 mm membranes. Mobile phase was 0.15M NaCl contained 0.02% NaN_3 (pH 7.0), at a flow rate of 0.5 mL/min.

2.6. Preparation of pectin gels

For cation-induced pectin gels, pectin samples were dissolved in distilled water under magnetic stirring for 3 h at 40 °C. In order to investigate the function of arabinose side-chains in gel formation, sample solutions containing different side-chain concentrations but the same backbone concentration were needed. Since GalA is the most stable component in pectin backbones, GalA content represents the concentration of backbones. The GalA contents (mol/g pectin; dry matter basis) of CP and DCP were different because of enzymatic debranching, so the concentration of the pectin solutions was adjusted to constant GalA content (0.3% (w/v)) (Ngouémazong et al., 2012; Sousa et al., 2015). As a result, pectin concentrations of CP and DCP were 1.28 and 0.71% (w/v). The pectin solutions were preheated at 60 °C and predetermined concentrations of Ca^{2+}, Mg^{2+}, Zn^{2+} and Na^{+}-ions (in solutions) were added dropwise under constant stirring to obtain homogeneous systems without pre-gelation. The preheated mixtures were put onto the rheometer and equilibrated for 5 min at 25 °C. Thereafter, the gels were analyzed for their rheological behavior. Different concentrations of cations were added to form pectin gels. Specific stoichiometric ratios ($R = 2\ [Ca^{2+}]/[COO^{-}]$) (Garnier, & Axelos, and Thibault, 1993) of 1–5.7 are required for the gelation of LM pectin in Ca^{2+}-induced pectin-gels and optimum gel stiffness was achieved at R-value of ~1.5–2.5 (Kyomugasho et al., 2016). Therefore, R = 0 (no added cations), 0.5, 1 and 2 were used with each pectin sample. The lower the R-value, the less calcium added. Taking into account that R-value is influenced by $[COO^{-}]$ and cation type, different amounts of cations were added depending on the DM, galacturonic acid content, pectin concentration, and the valence of the cation. Ca^{2+}-ion in each stoichiometric ratio was replaced with Mg^{2+}, Zn^{2+} and Na^{+}-ions where appropriate. For acid-induced pectin, pectin concentrations of CP and DCP solutions were the same as that of cation-induced gels. 1 wt% D-glucono-δ-lactone (GDL), 30 wt% sucrose and 1M urea were added as a dry powder to pectin solutions under constant stirring for 5 min to obtain homogeneous systems before the mixtures were put onto the rheometer for analysis (Fu & Rao, 2001; Liu, & Guo, & Li, & Zhu, and Li, 2013).

2.7. Rheological measurements

A HAAKE RheoStress 6000 rheometer (Thermo Scientific, USA) with a 40 mm parallel plate was used to analyze the rheological properties of pectins. Different solutions at GalA content of 0.4% and 0.2% (w/v)), for rheological tests were prepared by mixing pectins with distilled water under magnetic stirring for 3 h at 40 °C, resulting in pectin concentrations of 1.70 and 0.85% (w/v) for CP and concentrations of 0.94 and 0.47% (w/v) for DCP. The samples were subjected to steady shearing with the shear rates ranging from 0.1 to 100 s^{-1} at 25 °C. Data were fit to a power law model (equation (1)).

$$\eta = k\gamma^{(n-1)} \quad (1)$$

In equation (1), where η is the apparent viscosity (mPa•s), k (mPa•sn) is the consistency index, γ is the shear rate (s^{-1}) and n (dimensionless) is the flow behavior index. The linear viscoelastic ranges were determined by amplitude sweep from 0.001% to 100% at a constant angular frequency of 1 Hz. The angular frequency sweep was conducted from 0.1 to 10 Hz at 0.1% deformation (smaller than the maximum value of linear viscoelastic range) to monitor the change in storage modulus (G′) and loss modulus (G″) of the cation-pectin mixtures at 25 °C. The time-dependence of G′ and G″ were determined under 0.1% deformation and at constant angular frequency of 1 Hz for 10000s.

2.8. Visualization of microstructure of pectin gels (Cryo-SEM)

Cryo-scanning electron microscopy (Cryo-SEM) offers the most authentic insights into the native structure of polysaccharide hydrogels, due to the ability to freeze the sample under conditions where transparent vitreous ice is formed (Aston, & Sewell, & Klein, & Lawrie, and Grøndahl, 2016). A small amount of sample was first placed into a slot and cryo-vitrified with liquid nitrogen slush at −210 °C. Then, the vitrified sample was transferred to a cryo-SEM pre-chamber (PP3010T Cryo-SEM Preparation System, Quorum, UK) where free water was sublimated from the sample at −90 °C under vacuum conditions. After

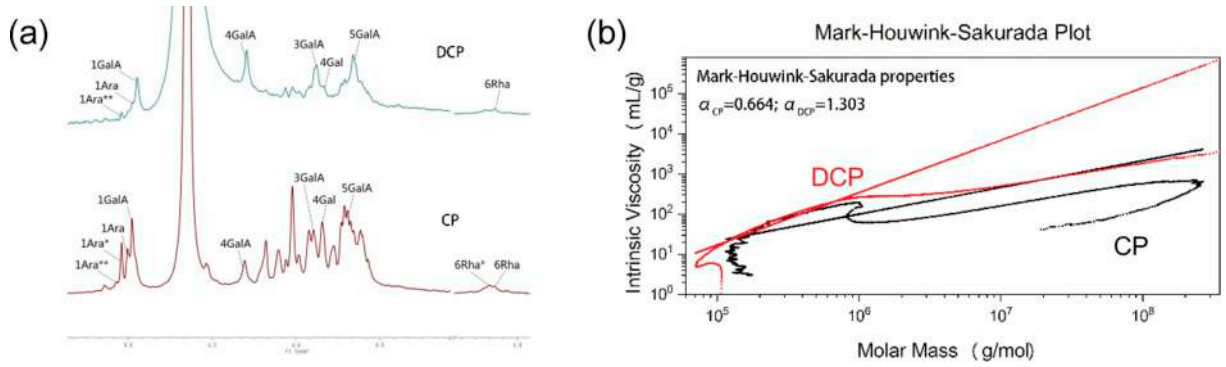

Fig. 1. (a) ^{1}H NMR spectrum of CP and DCP. (b) Chromatograms of chain conformation of CP and DCP in aqueous environment.

sublimation for 15–20 min, the sample was sputtered with gold to prevent charging during electron beam targeting. Finally, the sample was transferred on to the SEM stage (Regulus 8100, Hitachi, Japan) at −140 °C and the gel microstructure was observed (Kyomugasho et al., 2018; Ngouémazong et al., 2012).

2.9. Statistical analysis

Data were expressed as the mean ± standard deviation (SD) with three replicates per sample. Data were analyzed by ANOVA using Duncan's test with SPSS version 21.0 (IBM software, New York, USA). The significance level was set at $P < 0.05$.

3. Results and discussion

3.1. Structure of CP and DCP

The monosaccharide composition of citrus pectin (CP) revealed that sequential mild acid and alkaline extraction generates an RG-I like pectin, which is very different from HG dominated commercial pectins (Table 1). Arabinose, galacturonic acid, xylose, galactose and rhamnose are the major monosaccharide constituents, with a mole % of 43.27: 23.47: 12.82: 11.05: 4.19, suggesting that CP contains both RG-I (62.7%, mole % (2Rha + Ara + Gal)) and HG region (19.3%, mole % (GalA-Rha)) (Kazemi, & Khodaiyan, & Labbafi, & Saeid Hosseini, and Hojjati, 2019). Moreover, the high ratio of (Ara + Gal)/Rha suggested the RG-I portion has abundant Ara and Gal side-chains. According to the monosaccharide composition of enzymatically de-branched citrus pectin (DCP), enzymatic treatment removed 11.45% RG-I region. Significant reduction of (Ara + Gal)/Rha indicated degradation of neutral sugar side-chains while constant ratio of Rha and GalA suggested preservation of the HG and RG-I backbones. Determination of DM confirmed CP and DCP were both low-methoxylated pectin regarding the number of methyl-ester groups in HG region.

Values represent means ± standard derivatives of three replicates; values with different small case superscript letters in the same column indicate significant difference ($p < 0.05$), with the same letters indicate insignificant differences ($p > 0.05$).

Detailed structural information about the CP and DCP was obtained using ^{1}H NMR (Fig. 1a). Signals of GalA (H-1 4.98 ppm; H-2 3.69 ppm; H-3 3.90 ppm; H-4 4.31 ppm) were observed in both the CP and DCP spectra, confirming the remaining backbone (Zhi et al., 2017). CP contained both un-branched α-1,2-linked rhamnose (1.14 ppm) and branched α-1,2,4-linked rhamnose (1.17 ppm) while DCP mainly contained unbranched rhamnose (Sengkhamparn et al., 2009; Wang et al., 2016), indicating successful partial de-branching. Typical Ara signals in the DCP spectrum were smaller than those in the CP spectrum, especially H1 of un-branched α-1,5-linked arabinose (5.00 ppm) and branched α-1,3,5-linked arabinose (5.04 ppm), suggesting enzymatic de-branching removed both un-branched and branched arabinose. Signals of H2, H3, H4, H5, and H6 of galactose at 3.61–3.84 ppm indicated partial galactose reduction after enzymatic treatment (Zhou, & Huang, & Yue, and Ding, 2018).

SEC-MALLS-RI system gives accurate information for molecular size of a pectin sample. The Mw of CP was larger than DCP (Table 1), which conformed to the reduction of Ara and Gal shown by their monosaccharide compositions. Rz also decreased but to a lesser extent than Mw, indicating the "tighter" molecular structure of CP than DCP, and this "tight" structure is due to abundant neutral sugar side-chains in CP. The chain conformations of CP and DCP in 0.15 M NaCl solution was calculated by Mark-Houwink-Sakurada equation ($[\eta] = KM^{\alpha}$) (Fig. 1b). The exponent (α) of the equation with values of 0, 0–0.3, 0.5–0.8, 1 and 1.8–2 indicate a polymer is in a sphere, compacted coil, flexible chain, semi-flexible chain and rod-like rigid chain (Chaoyang et al., 2019).

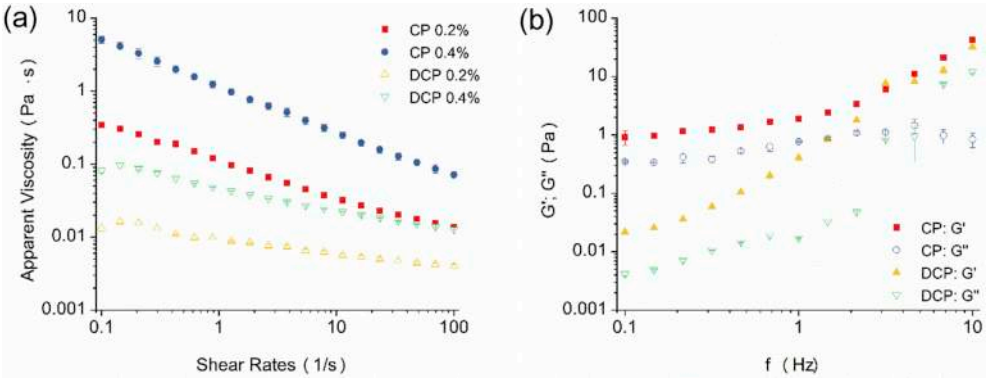

Fig. 2. (a) Apparent viscosity of CP and DCP at GalA concentration of 0.2% and 0.4% (w/v). (b) Storage modulus and loss modulus of CP and DCP at GalA concentration of 0.3% (w/v).

Table 2
Parameters of flow curves obtained by fitting to power law model.

Index	GalA Concentration			
	CP		DCP	
	0.20%	0.40%	0.20%	0.40%
k (mPa·s^n)	112.7	1172.4	9.6	47.8
n	1.488	1.626	1.205	1.302
R^2	0.996	0.999	0.977	0.990

According to the molecular weight of samples, the equation was used to evaluate the relationship between [η] and Mw in the region of 10^5–10^6 g/mol molar mass. Analysis showed that CP was in a flexible chain while DCP was semi-flexible. The main reason for this conformational change was ascribed to the partial removal of side-chains producing a more linear structure, thus, decreasing the flexibility of the polysaccharide chains.

3.2. *Effect of de-branching on steady shear flow behavior and dynamic-viscoelastic of pectin solution*

Steady shear flow behavior and dynamic-viscoelastic properties of CP and DCP were examined to investigate the effect of arabinose side-chains on the rheology properties of RG-I enriched pectin solution (Fig. 2). The viscosity of CP and DCP solutions both decreased with increasing shear rates (Fig. 2a), suggesting that they were both typical pseudoplastic fluids. This shear-thinning phenomenon is due to physical disruption of chain entanglements caused by steady shearing. Table 2 shows that the fitting accuracy of data points on the sample curve using the power law model reached 0.98, suggesting the model could be used to analysis CP and DCP samples. The consistency coefficient (K) and fluid index (n) were of magnitudes used to express fluid consistency and non-Newtonian fluid behavior in the model. Apparent viscosity increased with solution concentration, the possible explanation was high polysaccharide concentration decreased the distance between polymer chains and created more opportunities of inter-chain interactions, thus, leading to a higher apparent viscosity. The consistency coefficients of CP were higher than those of DCP at both concentrations, suggesting macromolecular entanglements of RG-I side-chains of CP lead to higher apparent viscosity. Fluid index slightly decreased with the diminution of concentration, indicating shear-thinning phenomenon is more obvious in high concentration solutions because freedom of movement of individual chains becomes restricted due to an increased amount of entanglements (Sousa et al., 2015). In terms of enzymatic treatment, the fluid index of DCP was lower than that of CP, indicating that the arabinose side-chains enhanced chain entanglements, therefore, restricting the movement of pectin chains.

Dynamic-viscoelastic properties of CP and DCP solutions are shown in Fig. 2b. Both CP and DCP solutions, appearing as thick liquids, should be considered to be weak gels because G′ was higher than the G′′

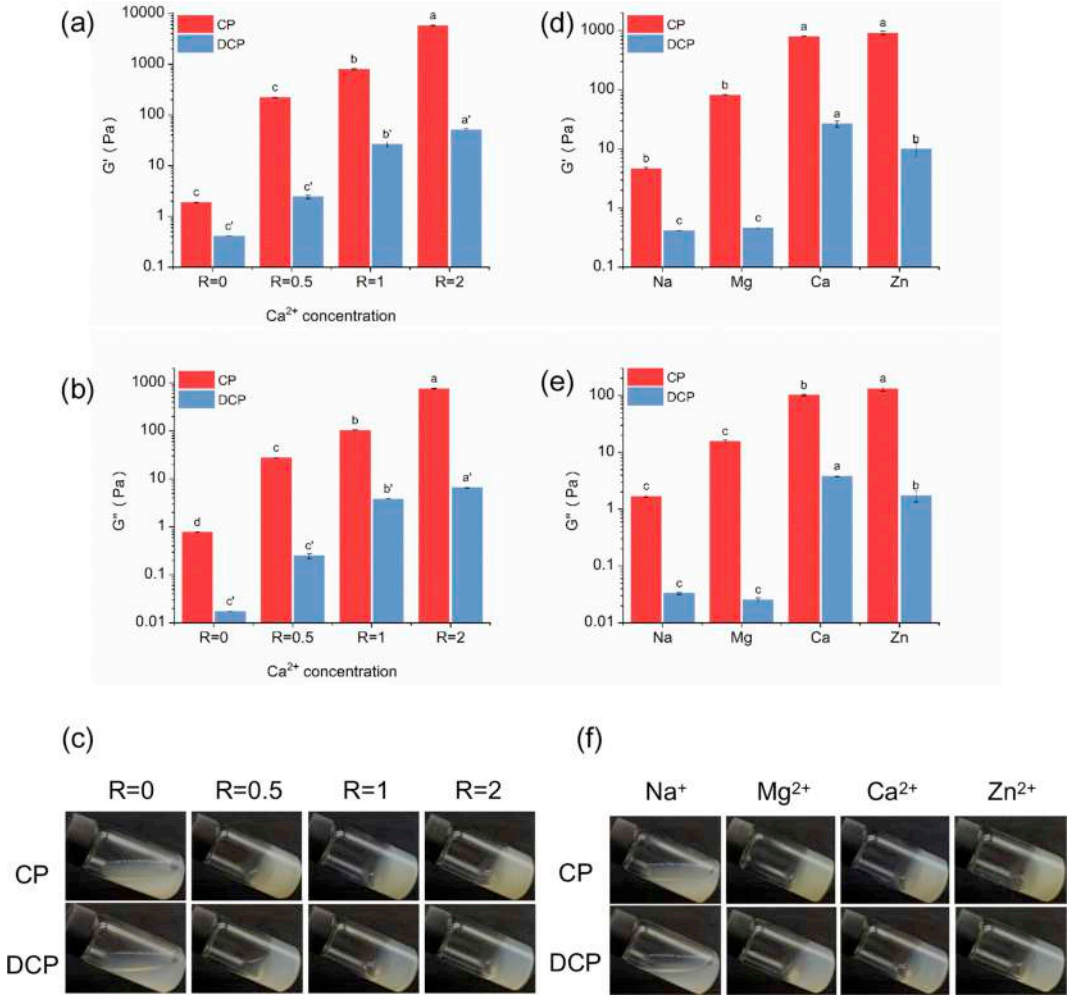

Fig. 3. Effect of R-value (R = 0, 0.5, 1 and 2) at 1 Hz on storage modulus (a) and loss (b) modulus of CP- and DCP-calcium mixtures. (c) Pictures of CP- and DCP-calcium mixtures at different R-value. Effect of cation types (Na^+, Mg^{2+}, Ca^{2+} and Zn^{2+}) on storage (d) and loss (e) modulus of CP- and DCP-cation mixtures with R = 1 at 1 Hz. (f) Picture of CP- and DCP-cation mixtures. GalA concentration = 0.6% (w/v).

(Kyomugasho et al., 2016). The dynamic moduli of DCP were lower than for CP and had more significant dependence on frequency, indicating the DCP is much more fluid-like than CP and the initial gel network in DCP solution was easily broken by oscillatory shear. One possible reason of the moduli dependency on frequency is that the pectin chains are arranged and stretched by oscillatory shear, thus, more sites become available to form intermolecular hydrogen bonds. Transformation from the intramolecular hydrogen bonds into intermolecular ones contributes to the formation of a three-dimensional network (Kjoniksen, & Hiorth, and Nystrom, 2005). In addition, moduli increased at a faster rate under high shear frequency, suggesting strong shear resulted in more obvious network rearrangement. The rheology properties of CP and DCP solutions indicate that CP appear as a weak gel in solution and that the arabinose side-chains of the RG-I region stabilize the network structure in the pectin solution.

The polymer concentration of DCP solutions was lower than that of CP solutions when maintaining a constant GalA content, because partial debranching resulted in an increase of the sample GalA content. In order to perform a reliable evaluation of the effect of side-chains, steady shear flow behavior and dynamic-viscoelastic properties of DCP 0.4% (0.94%, w/v) and that of CP 0.2% (0.85%, w/v) were compared. Even though DCP 0.4% contained more dry samples than CP 0.2%, the apparent viscosity was lower and dependence on frequency was more significant., which confirmed side-chains had major effect on rheology properties of RG-I enriched pectin. The major contribution of side-chians were also observed in RG-I enriched pectin gels (Ngouémazong et al., 2012; Sousa et al., 2015).

3.3. Effect of de-branching on dynamic-viscoelastic of cation-induced pectin gels

Pectin is an anionic polysaccharide that can interact with divalent cations through its nonmethylesterified galacturonic acid residues. Although Ca^{2+} is the most commonly used cation in pectin gelation, Zn^{2+} and Mg^{2+} were also explored for their ability to promote gelation. The storage modulus (Fig. 3a) and loss modulus (Fig. 3b) showed the rheology properties of the gels prepared from non-de-branched and de-branched RG-I enriched pectin, at three representative R values, i.e., R = 0.5, 1, and 2. Both G′ and G″ increased significantly with increasing R, the possible reason for this increase is that the addition of calcium ions allows cross-linking of non-methoxylated galacturonic acid residues. A "shifted" egg-box model is used to describe the network of Ca^{2+}-induced pectin gels, which is similar to the mechanism of alginate gelation. Electrostatic pectin-calcium interactions contribute to chain-chain association and one of the chains is slightly shifted with respect to the other, thus, generating junction zones in the pectin-calcium gels (Braccini & Perez, 2001). The number of Ca^{2+} ions at an R value of 0.5 could not match the amount required for complete gelation (Han et al., 2017), which is confirmed by pictures of gels (Fig. 3c) showing gel formation at R = 0.5 was not as complete as gels with higher R values. At low Ca^{2+} concentrations, point-like cross-links play a dominant role in gelation outside the egg-box junction zones. The point-like cross-links can occur between pectins with a relatively random distribution of non-methoxylated galacturonic acid and promote dimer formation (Zhang et al., 2019). Mathematically an R value of 1 means all non-methoxylated galacturonic acid residues can be bound with calcium ions, thus, egg-box junction zones are formed and G′ and G″ increase significantly. At R = 2, the Ca^{2+} concentration is well above the theoretical concentration of the egg-box model. The reason why G′ and G″ values of a gel at R = 2 are higher than those of a gel of R = 1 is that pectin-calcium interactions contribute to gel strength and that both junction zones and monocomplexes are formed in calcium-pectin gels (Ventura, & Jammal, and Bianco-Peled, 2013). Moreover, half of the non-methoxylated galacturonic acid residues are oriented towards the outside of the egg-boxes and can interact with additional calcium ions inducing the formation of larger dimer-dimer aggregates. However, formation of egg-boxes is only possible when non-methoxylated GalA residues are present in a sequence, the minimum length ranges from 6 to 14 GalA units. Accordingly, for RG-I enriched pectin, only the HG region is available for the egg-box formation, whereas, the backbone of RG-I region cannot even though it contains non-methoxylated GalA residues.

Moreover, the function of the side-chains of RG-I region in gelation is still unknown. The arabinose side-chains were removed by endo-α-1,5-arabinanase treatment and the rheology properties of DCP were determined to reveal the structure-gelation relationship of RG-I enriched pectin (Fig. 3). The increasing trend of gel strength with calcium addition in DCP was similar to that observed for CP, but the reduction of arabinose side-chains contributed to a reduction of more than 90% in G′ and G″ at both low and high R values. Since the same concentration of calcium was added into the CP- and DCP-Ca^{2+} gels containing an equivalent GalA content, the extremely low moduli observed in DCP-Ca^{2+} gels could be attributed to reduced Ca^{2+} dimerization of pectin chains due to the non-negligible reduction in the arabinose side-chains of DCP (Kyomugasho et al., 2016). In the shifted egg-box model, electrostatic interactions contribute to the strong chain-chain associations of dimers, in addition, two neighboring chains are stabilized by van der Waals interactions and hydrogen bonds, which involve hydroxyl groups at C2 and/or C3 at the inside faces of the dimers. Substitution at these sites, such as acetylation in sugar beet pectins, inhibits these interactions and decreases gelation ability. According to the gelation model, two possible roles of arabinose side-chains in RG-I enriched pectin gel are suggested, one is the side-chains act as substitution preventing the efficient packing of the chains, the other is they form entanglements through hydroxyl groups and strengthen the junction zones. The weakened gelation ability of DCP showed that the positive effect of arabinose side-chains in the gel is greater than the negative effect. The color of DCP gel was clearer than CP (Fig. 3c), suggesting that the aggregation of pectin chains in the DCP gel was less than that of the CP gel (Hua, & Yang, & Din, & Chi, and Yang, 2018), confirming that the arabinose side-chains were beneficial to pectin chain polymerization. The gel strength of CP increased significantly and the effect of R-value on DCP was much less than on CP. The higher calcium sensitivity of CP compared to DCP suggests that entanglements of arabinose side-chains promote the stabilization of chain-chain interactions and limit network chain mobility, thus, improving gel strength.

Zn^{2+} was selected to compare with the gelation ability of Ca^{2+} to further investigate the function of arabinose side-chains in RG-I enriched pectin gel. The shifted egg-box model was also used to describe the gelation of Zn^{2+}-pectin. The main difference between Ca^{2+} and Zn^{2+} was that Zn^{2+} interacted with both carboxyl and hydroxyl groups, whereas Ca^{2+} reportedly only binds through carboxyl groups (Assifaoui et al., 2014). Thus, arabinose side-chains could also connect with Zn^{2+} through their rich-hydroxyl group structure. Zinc was the most effective cation for CP gelation while calcium cation was most effective for DCP gelation (Fig. 3). The higher moduli of CP-Zn^{2+} gels demonstrates that arabinose side-chains stabilize gel formation by both intermolecular hydrogen bonds and electrostatic interactions due to this cation's ability to interact with hydroxyl groups.

The ability of arabinose side-chains to strengthen the chain-chain interactions in the egg box structure is confirmed in both Ca^{2+}-induced and Zn^{2+}-induced gels, however, some cation-induced pectin gels can form without an egg-box structure, such as those formed with Mg^{2+}. The main reason for this is that Mg^{2+} binds to pectin by polycondensation, due to its very high affinity for water, as a result, addition of Mg^{2+} is unable to build egg box structures in pectin like other divalent cations (Huynh, & Lerbret, & Neiers, & Chambin, and Assifaoui, 2016). Mono-coordination (such as that involving Mg^{2+}) is one of the most effective methods to improve gelation structure but these results are not as good as the junction zones formed with Ca^{2+} and Zn^{2+}. Due to the absent of egg box structures, Mg^{2+} showed a poorer gelation ability than Ca^{2+} and Zn^{2+} for both CP and DCP (Fig. 3). Moreover, G′ and G″ of CP-Mg^{2+} gels are higher than those of DCP-Mg^{2+} gels, indicating that

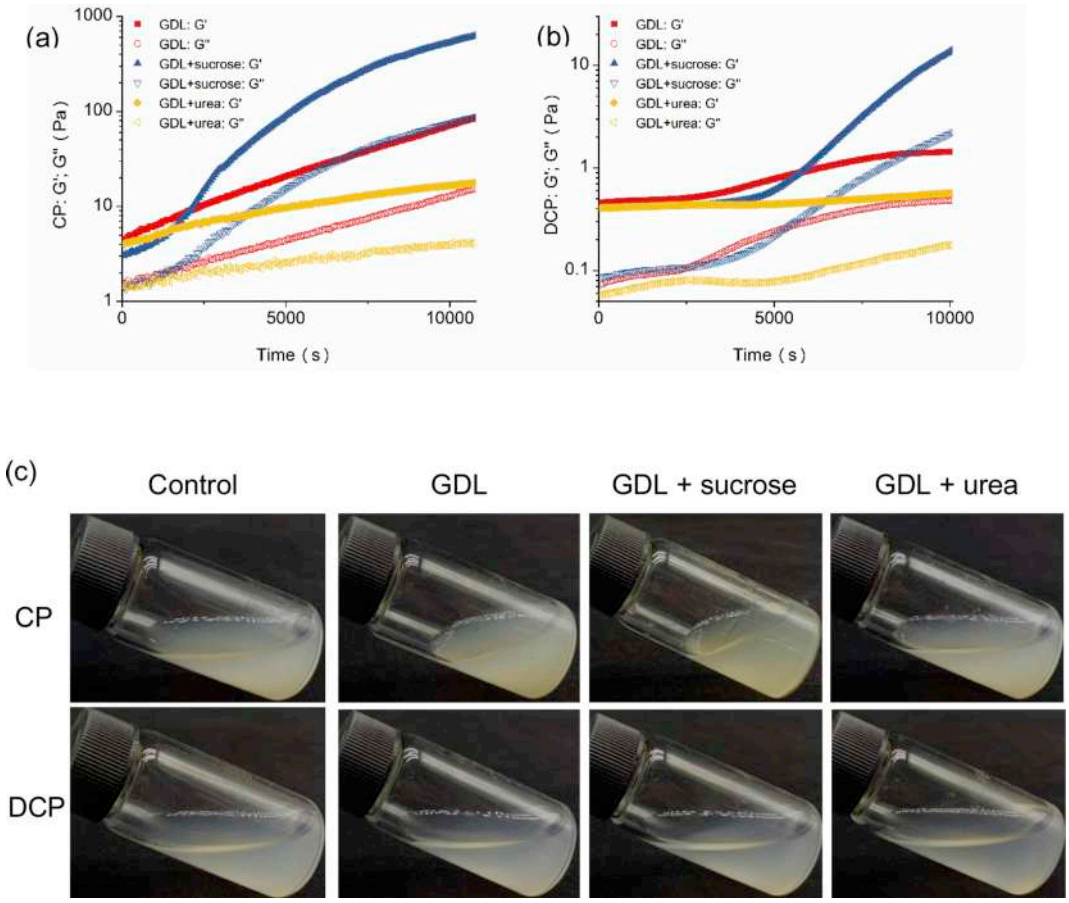

Fig. 4. Time-dependency of storage modulus (filled symbols) and loss (open symbols) modulus for CP- (a) and DCP- (b) with GDL 1%, GDL 1% + sucrose 30% and GDL1% + urea 1 M. GalA concentration = 0.6% (w/v). (c) Picture of CP-GDL and DCP-GDL mixtures with sucrose or urea.

arabinose side-chains stabilize gels without the egg box structures. Thus, arabinose side-chains can strengthen the chain-chain association even though the chains are not connected by cation-bridge.

The function of arabinose side-chains in monovalent cation-induced gelation was investigated using Na^+. Monovalent cations can also interact with carboxyl groups but the addition of Na^+ does not form a strong pectin gel. In contrast with divalent cations, monovalent cations bind with pectin chains to form mono-complexes. The addition of monovalent cations can hinder the electrostatic repulsion between pectin chains. This decrease of electrostatic repulsion reduces the distance between pectin chains and promotes the formation of hydrogen bonds. However, Na^+ reportedly does not completely diminish the electrostatic repulsion (Yapo, 2015), thus, addition of Na^+ results in a slight rise in the moduli of the mixtures for both CP and DCP but does not result in the formation of a stable gel (Fig. 3). The impact of Na^+ on CP gel strength is more obvious than its impact on DCP gel strength, indicating the initial distance between pectin chains of CP is shorter than that for DCP, consistent with the shortening of polymer chain distance and the formation of chain-chain interactions, resulting from the presence of arabinose side-chains.

3.4. *Effect of de-branching on dynamic-viscoelastic of acid-induced pectin gels*

Another important pectin gelation factor is pH. The mechanism of acid-induced gelation is a two-step process that depends on temperature. Hydrophobic interactions between the hydrophobic pectin methoxyl groups play a major role at temperatures above 50 °C, while hydrogen bonds between hydrophilic carboxyl and hydroxyl groups gradually replace the hydrophobic interactions on cooling (Chan, & Choo, & Young, and Loh, 2017; Einhorn-Stoll, 2018). At low pH values (below pH 3.5, the pKa value of pectin) protonation of carboxylic groups reduce electrostatic repulsions, thus, creating shorter distances between pectin chains resulting in bond formation. Pectin systems were acidified with 1% D-glucono-δ-lactone (GDL) and the dynamic moduli of CP-GDL (Fig. 4a) and DCP-GDL (Fig. 4b) mixtures were measured for 3 h at a constant stress of 0.1 Pa at 25 °C. The pH of CP solution was 4.47 ± 0.03, 3 h after addition of GDL, pH was 2.67 ± 0.05, while the pH of DCP was from 4.43 ± 0.01 to 2.66 ± 0.05. The G′ and G″ of CP-GDL mixture increased gradually as a function of time (Fig. 4a). The acid-induced gel was weak and flowable with clear and homogenous appearance 3h after addition of GDL (Fig. 4c), similar phenomenon observed in previous study (Han et al., 2017). Hydrogen bonds mainly contribute to gel formation of CP. CP is a low methoxyl pectin with high charge values, thus containing numerous active sites for hydrogen bonds formation. This leads to a great "connectivity" of the network and therefore to a high modulus (Yuliarti & Othman, 2018). The non-esterified carboxyl groups of RG-I enriched pectin backbone are converted to unionized with the hydrolysis of GDL, which can reduce the repulsion between pectin chains and prompt the formation of hydrophilic junction. In the case of arabinose side-chains, the moduli of DCP-GDL mixtures were much lower than those of CP-GDL mixtures, indicating arabinose side-chains prompt the formation of acid-induced networks. A possible explanation is the strong water-binding capacity of RG-I arabinan side chains inhibits the binding of water molecules with the hydroxyl groups of the HG structure and promotes the connection of pectin chains (Li et al., 2019). The entanglements of side-chains create a tighter conformation, which allowed for stronger hydrogen bonding of HG (Sousa et al., 2015). In addition, side-chain hydroxyl groups provide a large number of sites for hydrogen bonds, contributing to a stable network (Ngouémazong

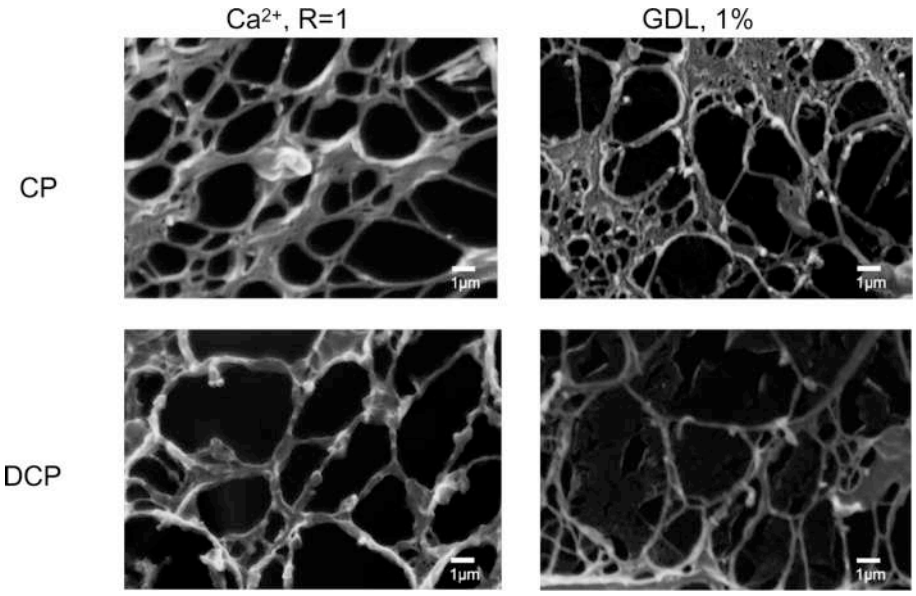

Fig. 5. Microstructure of calcium- and acid-induce pectin gels.

et al., 2012). G′ and G″ of DCP shows a discernible increase over a period of time after adding GDL, indicating a low pH sensitivity compared to CP, one possible interpretation is that the absence of arabinose side-chains increases the distance between pectin chains, thus, more hydrogen ions are required for the hydrogen bond work range (~0.2 nm).

Urea, a hydrogen bond destroyer (Huynh, Lerbret, Neiers, Chambin, & Assifaoui, 2016), was added in the CP-GDL and DCP-GDL mixtures to verify our hypothesis that the gelation of acid-induced RG-I enriched pectin gel mainly relies on hydrogen bonds and that the arabinose side-chains are important for such interaction formation The moduli of CP-GDL-urea system increased by lowering the pH, but the rate of growth was much lower than that of the CP-GDL system. For DCP, G′ was almost constant while G″ showed a small rise, indicating the addition of urea inhibits the network formation at low pH. This result provides compelling evidence to support the conclusion that acid-induced RG-I enriched pectin gel is a "physical gel" formed through chain association and particle aggregation involving mainly hydrogen bonding interactions (Yu et al., 2017). Other non-covalent cross-linking, such as hydrophobic and electrostatic interactions, may be present but their impact is limited. Comparing the results for the CP and DCP systems, addition of 1 M urea is sufficient to prevent the formation of acid-induced DCP gel, whereas the strength of CP-GDL-urea system still shows a small increase, confirming that the arabinose side-chains contribute more hydrogen bonds and stabilize the acid-induced RG-I enriched gel.

High concentrations of sucrose, or other cosolutes, are often required to form acid-induced pectin gels. Sucrose can preferentially interact with water due to its hydrophilicity and decrease the amount of water available to promote chain-chain interactions, such as hydrogen bonding and hydrophobic interactions (Fu & Rao, 2001). With addition of 30% sucrose, G′ and G″ of CP increase more than with the addition of only GDL. The growth rate of moduli suddenly increased about 2000 s after sucrose added, and a similar phenomenon has already been reported (Giacomazza, & Bulone, & San, & Marino, and Lapasin, 2018). One possible explanation is that the promotion effect of sucrose works when hydrogen bonding is sufficiently strong to create a three-dimensional network. In contrast with CP, the moduli of DCP-GDL-sucrose mixtures began to increase at 5000 s. This delay of time indicates a lower pH is required to form a three-dimensional network after removal of arabinose side-chains, implying that arabinose side-chains promote gel network formation, consistent with observation that the acid sensitivity of DCP is lower than CP. Rheology results confirm this (Fig. 4c), and the color of DCP systems is clearer than that of CP systems, suggesting less entanglement of pectin chains due to removal of the arabinose side-chains. Acid-induced RG-I enriched pectin gel mainly relies on hydrogen bonds junctions and arabinose side-chains promote three-dimensional network formation.

3.5. Microstructure of pectin gels

Cryo-SEM images of CP and DCP pectin gels with addition of calcium or GDL are shown in Fig. 5. For calcium-induced pectin gel (R = 1), an intertwined fibrous network was observed in both Ca^{2+}-induced CP and DCP gels, but the CP-Ca^{2+} gel has a denser and more highly cross-linked structure with smaller pores and thicker walls than the DCP-Ca^{2+} gel. The visual effect is consistent with the rheology properties (Fig. 3a, b), which indicate that the arabinose side-chains form additional junctions and enhance the entangle force (Liu et al., 2019). For acid-induced pectin gels, the cross-linked network in CP-GDL gel was out-of-order compared to CP-calcium gel. This phenomenon may explain the weak gel strength of acid-induced pectin (Fig. 4), suggesting different gelation mechanisms for cation- and acid-induced pectins. For DCP-GDL mixture, enzymatic de-branching results in large and open network structure. In contrast to CP-GDL gel, the dense structure almost disappears in DCP-GDL gel, suggesting that the flexible arabinose side-chains form entanglements and strengthen the acid-induced RG-I enriched gel. Arabinose side-chains of RG-I promote compact structure formation in both calcium and acid induced pectin gels and have a positive effect on gel strength.

3.6. Gelling mechanism of RG-I enriched citrus pectin

Approximately three-quarters of CP is composed of RG-I region with abundant arabinose side-chains and about one quarter of HG region and these different structures in pectin play different roles in its gelation. For cation-induced gelation, the free carboxyl groups of HG region on two adjacent pectin chains form an "egg box" structure with Ca^{2+} and the non-methoxylated galacturonic acid oriented towards the outside of the egg-boxes can form hydrogen bonds or interact with additional calcium ions, thus, inducing dimer-dimer interactions. In addition, the arabinose side-chains of RG-I enriched pectin can increase the space occupancy and shorten the distance between the pectin chains. Thus, additional entanglements are formed by hydrogen bonding interactions of

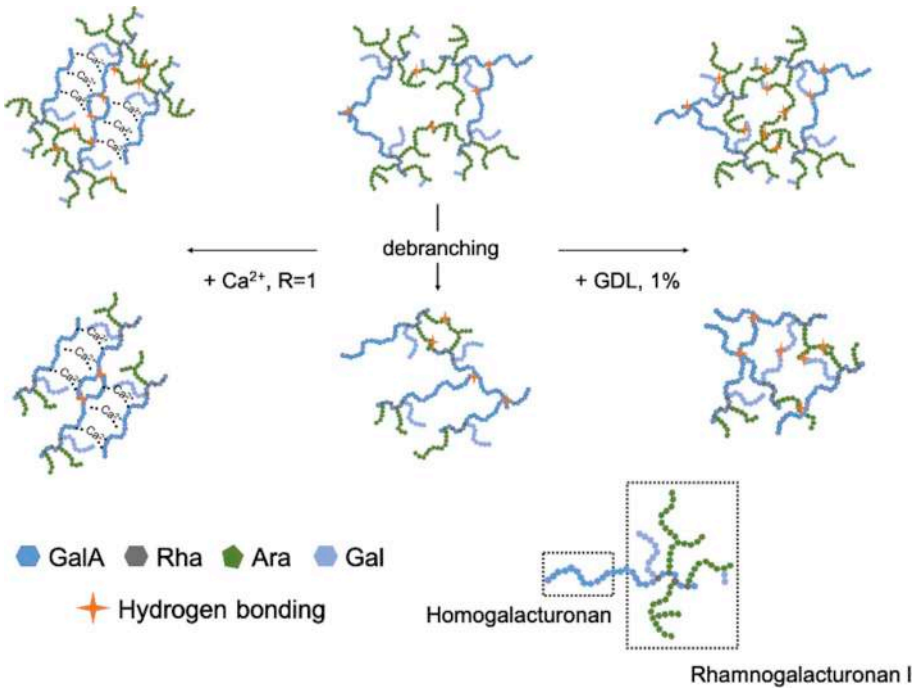

Fig. 6. Schematic diagram of the formation of RG-I enriched pectin network.

hydroxyl groups on the arabinose side-chains. The reduction of side-chains results in a decrease in entanglements, thus, limiting the formation of a gel network.

In acid-induced gelation, two typical junction zones in the gel have small working ranges of about 0.2 nm for hydrogen bonds and 2 nm for hydrophobic interactions compared to the 200 nm working ranges for the ionic junction zones (Einhorn-Stoll, 2018). Low pH protonates carboxylate residues, minimizing electrostatic repulsions and prompting junction zone formation. CP is inhomogeneous, composed of flexible RG-I region that contributes to a compact conformation and stiff rod-like HG region with an extended conformation. This complex structure leads to different distances between polysaccharide chains in the gel system. As a result, partial pectin chains are in close contact with each other and form bonds but others cannot because of the long chain-to-chain distances, resulting in the inhomogeneous microstructure and relatively weak gel properties of acid-induced gels. The arabinose side-chains have strong water-binding capacity, thus, promoting the connection of pectin chains through hydrophobic interactions and hydrogen bonding. In addition, side-chain entanglements restrict the mobility of pectin molecules and create a stable gel network. After enzymatic de-branching, side-chain entanglements decrease and pectin molecule conformation becomes looser, inhibiting gel formation (see Fig. 6).

4. Conclusions

In this study, rheological method and Cryo-SEM imaging were used to elucidate the gelation mechanism of RG-I enriched pectin from citrus membrane (CP), especially the role of arabinose side-chains. CP contains more than 70% RG-I regions, with abundant neutral sugar side-chains mainly composed of arabinan, thus, CP has a special gelation mechanism different from commercial pectin. In cation-induced gelation, abundant divalent cations such as Ca^{2+} and Zn^{2+} generally interact with carboxyl groups on galacturonic acid of HG region and form egg-box junction zones, side-chains of the RG-I region stabilize both the chain-chain and dimer-dimer structures through entanglements. These entanglements make the gel network denser and limit network chain mobility, thus, improving gel strength. For acid-induced gelation, low pH promotes the formation of hydrogen bonds and hydrophobic interactions between pectin chains and the side-chains play an active role in hydrogen bond interactions to strengthen the gel network. Moreover, side-chain entanglements create a tighter conformation, eventually allowing for stronger hydrophobic interactions and hydrogen bonding in HG. In summary, RG-I enriched pectin with abundant arabinose sugar side-chains can form gels under both cation and acid conditions and its side-chains improve network formation. The experimental results obtained from this work form the basis for the further optimization of gelation conditions and the future applications of RG-I enriched pectins.

Declaration of competing interest

The authors declare that we do not have any commercial or associative interest that represents a conflict of interest in connection with the work submitted.

Acknowledgements

This work was financially supported by National Key R&D Program of China (2017YFE0122300) and National Natural Science Foundation of China (31871815).

Appendix A. Supplementary data

Supplementary data to this article can be found online at https://doi.org/10.1016/j.foodhyd.2019.105536.

References

Assifaoui, A., Lerbret, A., Uyen, H. T., Neiers, F., Chambin, O., Loupiac, C., et al. (2014). Structural behaviour differences in low methoxy pectin solutions in the presence of divalent cations (Ca^{2+} and Zn^{2+}): A process driven by the binding mechanism of the cation with the galacturonate unit. *Soft Matter, 11*(3), 551–560.

Aston, R., Sewell, K., Klein, T., Lawrie, G., & Grøndahl, L. (2016). Evaluation of the impact of freezing preparation techniques on the characterisation of alginate hydrogels by cryo-SEM. *European Polymer Journal, 82*, 1–15.

Babbar, N., Dejonghe, W., Gatti, M., Sforza, S., & Elst, K. (2016). Pectic oligosaccharides from agricultural by-products: Production, characterization and health benefits. *Critical Reviews in Biotechnology, 36*(4), 594.

Barbieri, S. F., Amaral, S. D. C., Ruthes, A. C., de Oliveira Petkowicz, C. L., Kerkhoven, N. C., Silva, E. R. A. D., et al. (2019). Pectins from the pulp of gabiroba (Campomanesia xanthocarpa Berg): Structural characterization and rheological behavior. *Carbohydrate Polymers, 214*, 250–258.

Braccini, I., & Perez, S. (2001). Molecular basis of Ca^{2+}-induced gelation in alginates and pectins: The egg-box model revisited. *Biomacromolecules, 2*(4), 1089–1096.

Chan, S. Y., Choo, W. S., Young, D. J., & Loh, X. J. (2017). Pectin as a rheology modifier: Origin, structure, commercial production and rheology. *Carbohydrate Polymers, 161*, 118–139.

Chaoyang, W., Yu, Z., Hua, Z., Junhui, L., Wenyang, T., Linhardt, R. J., et al. (2019). Physicochemical properties and conformations of water-soluble peach gums via different preparation methods. *Food Hydrocolloids, 95*, 571–579.

Chen, J., Chen, W., Duan, F., Tang, Q., Li, X., Zeng, L., et al. (2019). The synergistic gelation of okra polysaccharides with kappa-carrageenan and its influence on gel rheology, texture behaviour and microstructures. *Food Hydrocolloids, 87*, 425–435.

Chen, J., Cheng, H., Wu, D., Linhardt, R. J., Zhi, Z., Yan, L., et al. (2017). Green recovery of pectic polysaccharides from citrus canning processing water. *Journal of Cleaner Production, 144*, 459–469.

Einhorn-Stoll, U. (2018). Pectin-water interactions in foods - from powder to gel. *Food Hydrocolloids, 78*, 109–119.

Fraeye, I., Duvetter, T., Doungla, E., Van Loey, A., & Hendrickx, M. (2010). Fine-tuning the properties of pectin–calcium gels by control of pectin fine structure, gel composition and environmental conditions. *Trends in Food Science & Technology, 21*(5), 219–228.

Fu, J., & Rao, M. A. (2001). Rheology and structure development during gelation of low-methoxyl pectin gels: The effect of sucrose. *Food Hydrocolloids, 15*(1), 93–100.

Garnier, C., Axelos, M. A. V., & Thibault, J. (1993). Phase diagrams of pectin-calcium systems: Influence of pH, ionic strength, and temperature on the gelation of pectins with different degrees of methylation. *Carbohydrate Research, 240*, 219–232.

Giacomazza, D., Bulone, D., San, B. P., Marino, R., & Lapasin, R. (2018). The role of sucrose concentration in self-assembly kinetics of high methoxyl pectin. *International Journal of Biological Macromolecules, 112*, 1183–1190.

Gunning, A. P., Bongaerts, R. J., & Morris, V. J. (2009). Recognition of galactan components of pectin by galectin-3. *The FASEB Journal, 23*(2), 415–424.

Günter, E. A., Popeyko, O. V., & Istomina, E. I. (2019). Encapsulated drug system based on the gels obtained from callus cultures modified pectins. *Journal of Biotechnology, 289*, 7–14.

Han, W., Meng, Y., Hu, C., Dong, G., Qu, Y., Deng, H., et al. (2017). Mathematical model of Ca^{2+} concentration, pH, pectin concentration and soluble solids (sucrose) on the gelation of low methoxyl pectin. *Food Hydrocolloids, 66*, 37–48.

Hua, X., Yang, H., Din, P., Chi, K., & Yang, R. (2018). Rheological properties of deesterified pectin with different methoxylation degree. *Food Bioscience, 23*, 91–99.

Huynh, U. T., Lerbret, A., Neiers, F., Chambin, O., & Assifaoui, A. (2016). Binding of divalent cations to polygalacturonate: A mechanism driven by the hydration water. *Journal of Physical Chemistry B, 120*(5), 1021–1032.

Kapoor, S., & Dharmesh, S. M. (2017). Pectic Oligosaccharide from tomato exhibiting anticancer potential on a gastric cancer cell line: Structure-function relationship. *Carbohydrate Polymers, 160*, 52–61.

Kazemi, M., Khodaiyan, F., Labbafi, M., Saeid Hosseini, S., & Hojjati, M. (2019). Pistachio green hull pectin: Optimization of microwave-assisted extraction and evaluation of its physicochemical, structural and functional properties. *Food Chemistry, 271*, 663–672.

Khodaei, N., & Karboune, S. (2013). Extraction and structural characterisation of rhamnogalacturonan I-type pectic polysaccharides from potato cell wall. *Food Chemistry, 139*(1–4), 617–623.

Khodaei, N., & Karboune, S. (2014). Enzymatic extraction of galactan-rich rhamnogalacturonan I from potato cell wall by-product. *Lebensmittel-Wissenschaft und -Technologie- Food Science and Technology, 57*(1), 207–216.

Kjoniksen, A. L., Hiorth, M., & Nystrom, B. (2005). Association under shear flow in aqueous solutions of pectin. *European Polymer Journal, 41*(4), 761–770.

Kyomugasho, C., Christiaens, S., Van de Walle, D., Van Loey, A. M., Dewettinck, K., & Hendrickx, M. E. (2016). Evaluation of cation-facilitated pectin-gel properties: Cryo-SEM visualisation and rheological properties. *Food Hydrocolloids, 61*, 172–182.

Kyomugasho, C., Munyensanga, C., Celus, M., Van de Walle, D., Dewettinck, K., Van Loey, A. M., et al. (2018). Molar mass influence on pectin-Ca^{2+} adsorption capacity, interaction energy and associated functionality: Gel microstructure and stiffness. *Food Hydrocolloids, 85*, 331–342.

Levigne, S., Thomas, M., Ralet, M. C., Quemener, B., & Thibault, J. F. (2002). Determination of the degrees of methylation and acetylation of pectins using a C18 column and internal standards. *Food Hydrocolloids, 16*(6), 547–550.

Li, X., Dong, Y., Guo, Y., Zhang, Z., Jia, L., Gao, H., et al. (2019). Okra polysaccharides reduced the gelling-required sucrose content in its synergistic gel with high-methoxyl pectin by microphase separation effect. *Food Hydrocolloids, 95*, 506–516.

Liu, H., Guo, X., Li, J., Zhu, D., & Li, J. (2013). The effects of MgSO4, d-glucono-δ-lactone (GDL), sucrose, and urea on gelation properties of pectic polysaccharide from soy hull. *Food Hydrocolloids, 31*(2), 137–145.

Liu, S., Xiao, Y., Shen, M., Zhang, X., Wang, W., & Xie, J. (2019). Effect of sodium carbonate on the gelation, rheology, texture and structural properties of maize starch-Mesona chinensis polysaccharide gel. *Food Hydrocolloids, 87*, 943–951.

Li, H., Yang, S., Li, J., & Feng, J. (2018). Galectin 3 inhibition attenuates renal injury progression in cisplatin-induced nephrotoxicity. *Bioscience Reports, 38*(6).

Makshakova, O. N., Faizullin, D. A., Mikshina, P. V., Gorshkova, T. A., & Zuev, Y. F. (2018). Spatial structures of rhamnogalacturonan I in gel and colloidal solution identified by 1D and 2D-FTIR spectroscopy. *Carbohydrate Polymers, 192*, 231–239.

Maxwell, E. G., Belshaw, N. J., Waldron, K. W., & Morris, V. J. (2012). Pectin – an emerging new bioactive food polysaccharide. *Trends in Food Science & Technology, 24*(2), 64–73.

Mikshina, P. V., Makshakova, O. N., Petrova, A. A., Gaifullina, I. Z., Idiyatullin, B. Z., Gorshkova, T. A., et al. (2017). Gelation of rhamnogalacturonan I is based on galactan side chain interaction and does not involve chemical modifications. *Carbohydrate Polymers, 171*, 143–151.

Ngouémazong, D. E., Kabuye, G., Fraeye, I., Cardinaels, R., Van Loey, A., Moldenaers, P., et al. (2012). Effect of debranching on the rheological properties of Ca^{2+}–pectin gels. *Food Hydrocolloids, 26*(1), 44–53.

Sandarani, M. (2017). *A review: Different extraction techniques of pectin* (Vol. 3, pp. 1–5). OMICS International.

Schmelter, T., Wientjes, R., Vreeker, R., & Klaffke, W. (2002). Enzymatic modifications of pectins and the impact on their rheological properties. *Carbohydrate Polymers, 47*(2), 99–108.

Sengkhamparn, N., Bakx, E. J., Verhoef, R., Schols, H. A., Sajjaanantakul, T., & Voragen, A. G. J. (2009). Okra pectin contains an unusual substitution of its rhamnosyl residues with acetyl and alpha-linked galactosyl groups. *Carbohydrate Research, 344*(14), 1842–1851.

Sousa, A. G., Nielsen, H. L., Armagan, I., Larsen, J., & Sørensen, S. O. (2015). The impact of rhamnogalacturonan-I side chain monosaccharides on the rheological properties of citrus pectin. *Food Hydrocolloids, 47*, 130–139.

Strydom, D. J. (1994). Chromatographic separation of 1-phenyl-3-methyl-5-pyrazolone-derivatized neutral, acidic and basic aldoses. *Journal of Chromatography A, 678*(1), 17–23.

Ventura, I., Jammal, J., & Bianco-Peled, H. (2013). Insights into the nanostructure of low-methoxyl pectin–calcium gels. *Carbohydrate Polymers, 97*(2), 650–658.

Wang, W., Ma, X., Jiang, P., Hu, L., Zhi, Z., Chen, J., et al. (2016). Characterization of pectin from grapefruit peel: A comparison of ultrasound-assisted and conventional heating extractions. *Food Hydrocolloids, 61*, 730–739.

Willats, W., Knox, P., & Mikkelsen, J. D. (2006). Pectin: New insights into an old polymer are starting to gel. *Trends in Food Science & Technology, 17*(3), 97–104.

Wu, D., Zheng, J., Mao, G., Hu, W., Ye, X., Linhardt, R. J., & Chen, S. (2019). Rethinking the impact of RG-I mainly from fruits and vegetables on dietary health. *Critical Reviews in Food Science and Nutrition*, 1–23. https://doi.org/10.1080/10408398.2019.1672037.

Yapo, B. M. (2011). Rhamnogalacturonan-I: A structurally puzzling and functionally versatile polysaccharide from plant cell walls and mucilages. *Polymer Reviews, 51*(4), 391–413.

Yapo, B. M. A. G. (2015). *Pectic polysaccharides and their functional properties*. Cham: Springer International Publishing.

Yapo, B. M., Robert, C., Etienne, I., Wathelet, B., & Paquot, M. (2007). Effect of extraction conditions on the yield, purity and surface properties of sugar beet pulp pectin extracts. *Food Chemistry, 100*(4), 1356–1364.

Yuliarti, O., & Othman, R. M. B. (2018). Temperature dependence of acid and calcium-induced low-methoxyl pectin gel extracted from Cyclea barbata Miers. *Food Hydrocolloids, 81*, 300–311.

Yu, L., Yakubov, G. E., Zeng, W., Xing, X., Stenson, J., Bulone, V., et al. (2017). Multi-layer mucilage of Plantago ovata seeds: Rheological differences arise from variations in arabinoxylan side chains. *Carbohydrate Polymers, 165*, 132–141.

Zhang, H., Chen, J., Li, J., Yan, L., Li, S., Ye, X., et al. (2017). Extraction and characterization of RG-I enriched pectic polysaccharides from Mandarin citrus peel. *Food Hydrocolloids, 79*.

Zhang, B., Hu, B., Nakauma, M., Funami, T., Nishinari, K., Draget, K. I., et al. (2019). Modulation of calcium-induced gelation of pectin by oligoguluronate as compared to alginate. *Food Research International, 116*, 232–240.

Zhao, J., Zhang, F., Liu, X., St, A. K., Zhang, A., Li, Q., et al. (2017). Isolation of a lectin binding rhamnogalacturonan-I containing pectic polysaccharide from pumpkin. *Carbohydrate Polymers, 163*, 330–336.

Zhi, Z., Chen, J., Li, S., Wang, W., Huang, R., Liu, D., et al. (2017). Fast preparation of RG-I enriched ultra-low molecular weight pectin by an ultrasound accelerated Fenton process. *Scientific Reports, 7*(1), 541.

Zhou, L., Huang, L., Yue, H., & Ding, K. (2018). Structure analysis of a heteropolysaccharide from fruits of Lycium barbarum L. and anti-angiogenic activity of its sulfated derivative. *International Journal of Biological Macromolecules, 108*, 47–55.